ACS OMEGA

http://pubs.acs.org/journal/acsodf

Article

Core Constituents of *Caragana sinica Root* for Rheumatoid Arthritis Treatment and the Potential Mechanism

Biao Qu,[†] Shimin Wang,[†] Hailan Zhu,[†] Tianpeng Yin, Renpeng Zhou, Wei Hu,* and Chao Lu*

Cite This: *ACS Omega* 2023, 8, 2586−2595

Read Online

ACCESS | Metrics & More | Article Recommendations | Supporting Information

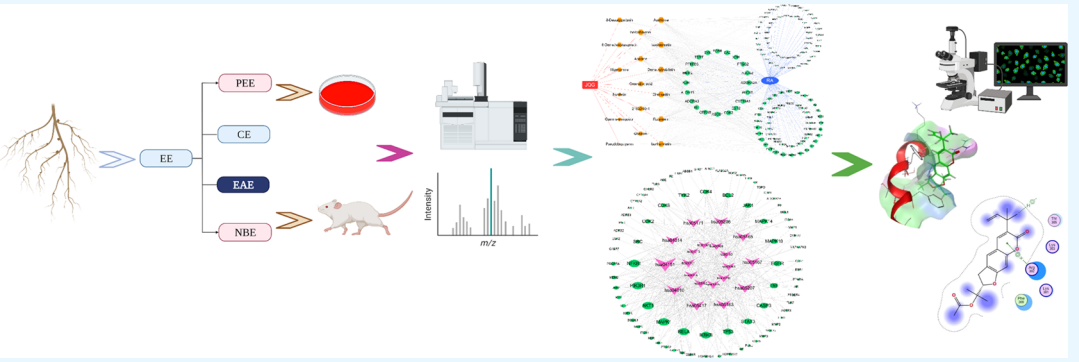

ABSTRACT: Purpose: As a traditional herb product, the root of *Caragana sinica (Buc'hoz) Rehder* (Chinese name: Jin Quegen [JQG]) has been widely used in folk medicines for rheumatoid arthritis (RA) treatment. However, which herbal constituents exert a core pharmacological role in RA treatment remains a great challenge due to the multiple phytochemical constituents, targets, and pathways. In this work, we aimed to use a new strategy to explore the core herbal constituents and potential mechanisms of JQG against RA for the first time. Methods: A successively partitioned extract of JQG, bioactive partition screening in vitro and in vivo, qualitative analysis, bioinformatic analysis, molecular docking, and mechanism validation were used in this study. The partitioned extract was used to obtain the bioactive partition, while in vitro anti-inflammatory effects and in vivo anti-arthritis effects in adjuvant-induced arthritis (AIA) rats were applied to screen the bioactive partition with the best efficacy. Qualitative analysis was used to identify bioactive constituents. Bioinformatic analysis was used to explore the potential mechanism for RA treatment. Molecular docking and immunofluorescence were used to validate the underlying mechanism. Results: After successively partitioning extract and bioactive partition screening, ethyl acetate extract (EAE) yielded the best anti-inflammatory effects in vitro and in vivo among JQG extracts. By ultra-performance liquid chromatography (UPLC) coupled with Orbitrap mass spectrometry, a total of 58 constituents were identified in EAE, and 17 constituents were regarded as the core constituents based on their oral bioavailability and drug-like properties. The nuclear factor kappa B (NF-κB) signal pathway was screened as the core pathway of core constituents for RA treatment based on bioinformatic analysis, and the core constituents showed good ligand−receptor binding activity to NF-κB P65. In vitro study demonstrated that EAE could significantly reduce NF-κB P65 transfer from the cytoplasm to the nucleus. Conclusion: Our study suggested that the therapeutic efficacy of JQG for RA treatment could be derived from negative regulation of the NF-κB pathway, and EAE of JQG could represent a promising herb product for RA treatment that deserves further development.

1. INTRODUCTION

Rheumatoid arthritis (RA) is a chronic systemic inflammatory disease characterized by erosive synovitis that can cause severe joint destruction and disability,[1,2] as well as the involvement of other tissues throughout the body.[3] Disease-modifying anti-rheumatic drugs (DMARDs), biological DMARDs, and herbal products represent the most important agents to alleviate symptoms and prevent RA progression.[4,5] Traditional Chinese medicines have been widely applied to disease treatment, cosmetics, and health care products.[6] Many of the drugs used in clinical practice are directly or indirectly derived from traditional Chinese medicines.[7] Traditional Chinese medicine has the characteristic of a multiconstituent, multitarget, and multipathway treatment,[8] which has shown great efficacy and mild adverse effects in RA prevention and treatment.[9,10] *Caragana sinica root* (Chinese name: Jin Quegen [JQG]), the dried root of *Caragana sinica (Buc'hoz) Rehder (Leguminosae)*, is widely distributed in China, Korea, and Japan.[11] JQG has been used as a folk medicine in China and Korea for the

Received: November 4, 2022
Accepted: December 23, 2022
Published: January 5, 2023

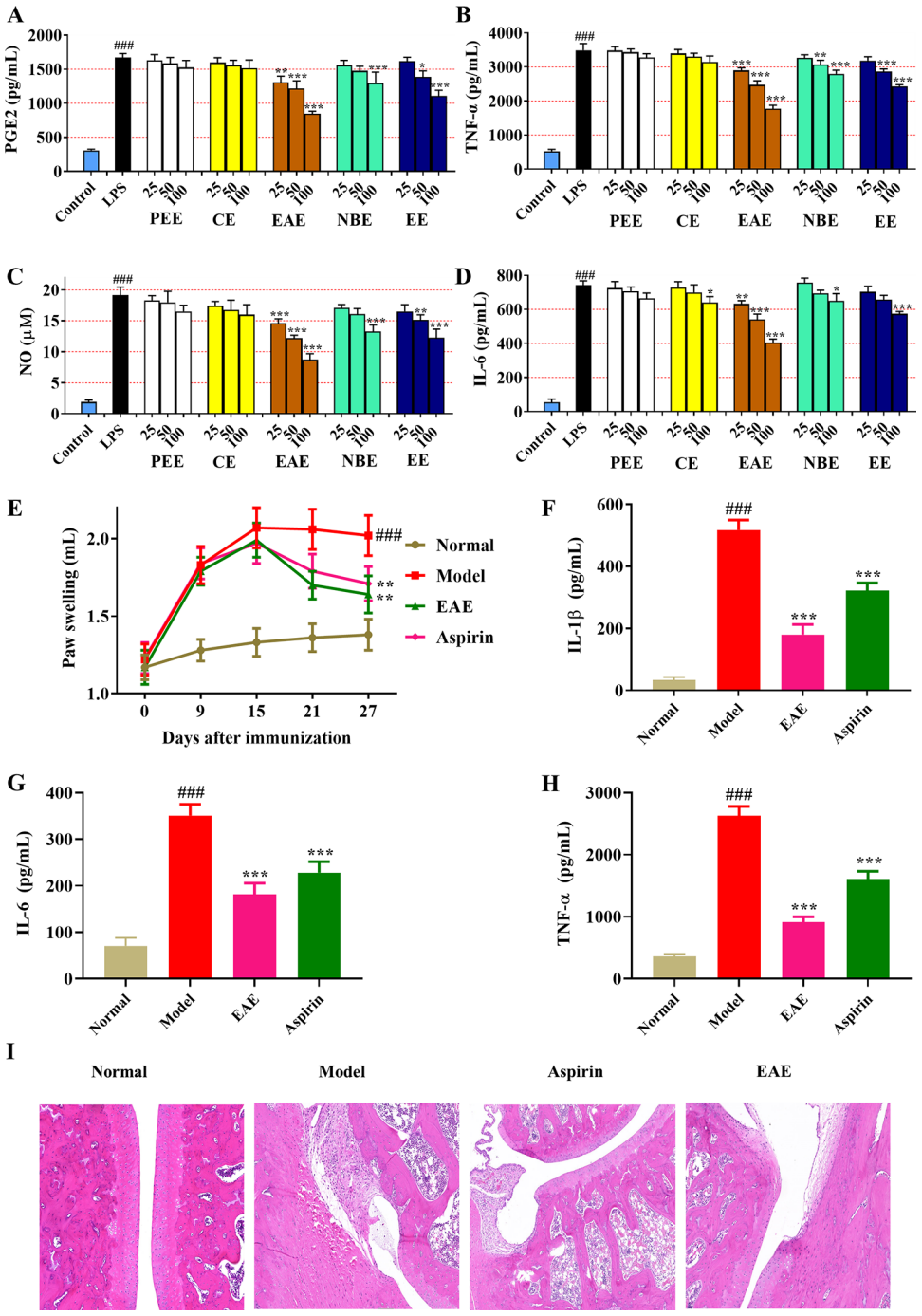

Figure 1. Anti-inflammatory effects of different JQG extracts on RAW264.7 cells and AIA rats. Concentrations of (A) PGE2, (B) TNF-α, (C) NO, and (D) IL-6 in RAW264.7 cells stimulated with 1 μg/mL LPS (n = 3). The doses of EE, PEE, CE, EAE, and NBE were 25, 50, and 100 μg/mL. All data are displayed as the mean ± SD. * p < 0.01, ** p < 0.01, *** p < 0.001 vs LPS-stimulated cells, ### p < 0.001 vs unstimulated cells. Anti-arthritic effects of JQG EAE on AIA rats (n = 5). (E) Effect of EAE on the swelling of the left hind paw of AIA rats. Effect of EAE on the secretion of serum inflammatory cytokines (F) interleukin-1 beta (IL-1β), (G) IL-6, and (H) TNF-α in AIA rats; (I) hematoxylin and eosin (H&E) staining of ankle joints of AIA rats (×100). ** p < 0.01, *** p < 0.001 vs the control group; ### p < 0.001 vs the model group.

treatment of neuralgia, RA, vascular hypertension, and bruises.[12,13] Clinically, JQG not only yields good efficacy for RA treatment but also has a very high safety profile.[14,15]

JQG has demonstrated antioxidative, neuroprotective, antibacterial, anti-inflammatory, neuroprotective effects, and *anti*-acetylcholinesterase activity.[16−20] Phytochemical analyses have indicated that JQG mainly contains triterpenoids, flavonoids, oligostilbene, alkaloids, sesquiterpenoids, pterostilbene, steroidal phenylpropanoid, and coumarin.[12,21−23] However, there are multiple constituents in JQG, and many of them have been reported to exhibit biological activities. Additionally, multiple constituents can work synergistically on the targets to produce an overall therapeutic effect. Therefore, exploring which constituents make a core contribution to the efficacy of JQG is a huge challenge. The same problem makes it difficult to elucidate the relationship between phytochemicals and overall efficacy. Furthermore, almost all studies have focused

https://doi.org/10.1021/acsomega.2c07094
ACS Omega 2023, 8, 2586−2595

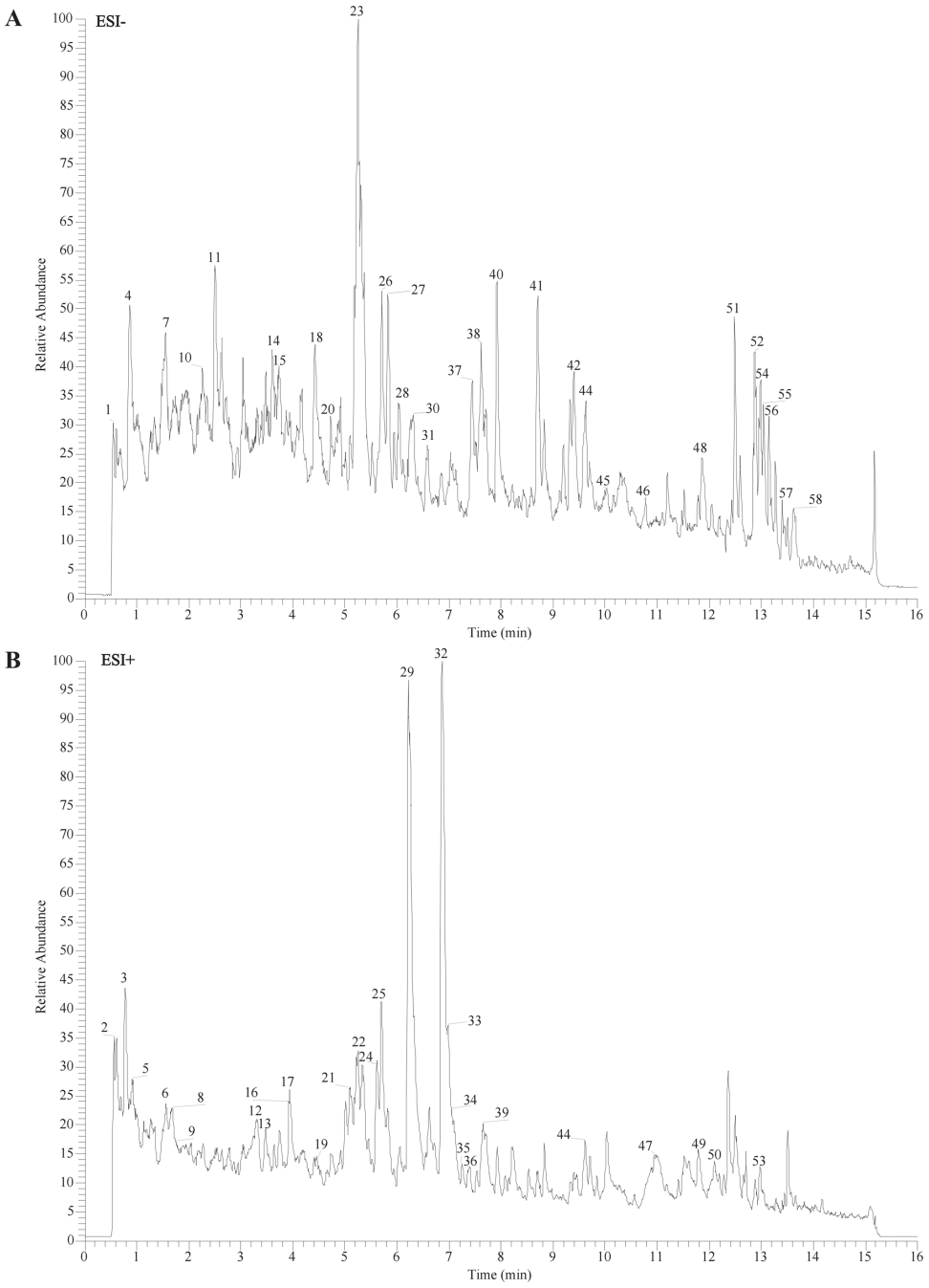

Figure 2. TICs of JQG EAE obtained from UPLC coupled Orbitrap Exploris 120 mass spectrometer analysis in (A) negative mode and (B) positive mode.

on the isolated constituents and pharmacological activity rather than the precise mechanism of JQG for RA therapy.

Due to the complex chemical constituents of Chinese medicines, it is difficult for traditional research methods to fully elucidate the mechanism of Chinese medicines. Therefore, it is of high necessity to provide a method for this problem solution, which is suitable for the study of multiconstituent and multitarget compounds in traditional Chinese medicine. Network pharmacology is an emerging discipline based on an organic combination of systems biology, computer technology, pharmacology, and medicine. Based on bioinformatics, a multilevel network of disease−target−drug interactions can be constructed, followed by the analysis of the association between them, to clarify the mechanism of drugs on diseases at the protein, molecular, and gene levels.[24−26]

In this work, an integrative strategy combining successively partitioned extraction of JQG, bioactive partition screening in vitro and in vivo, qualitative analysis, bioinformatic analysis, molecular docking, and mechanism validation were used to exploit the core active constituents and potential mechanism of JQG for RA treatment.

2. RESULTS

2.1. Screening of Bioactive Partition of JQG Extract. The anti-inflammatory effects of ethanol extract (EE), petroleum ether extract (PEE), chloroform extract (CE),

https://doi.org/10.1021/acsomega.2c07094
ACS Omega 2023, 8, 2586−2595

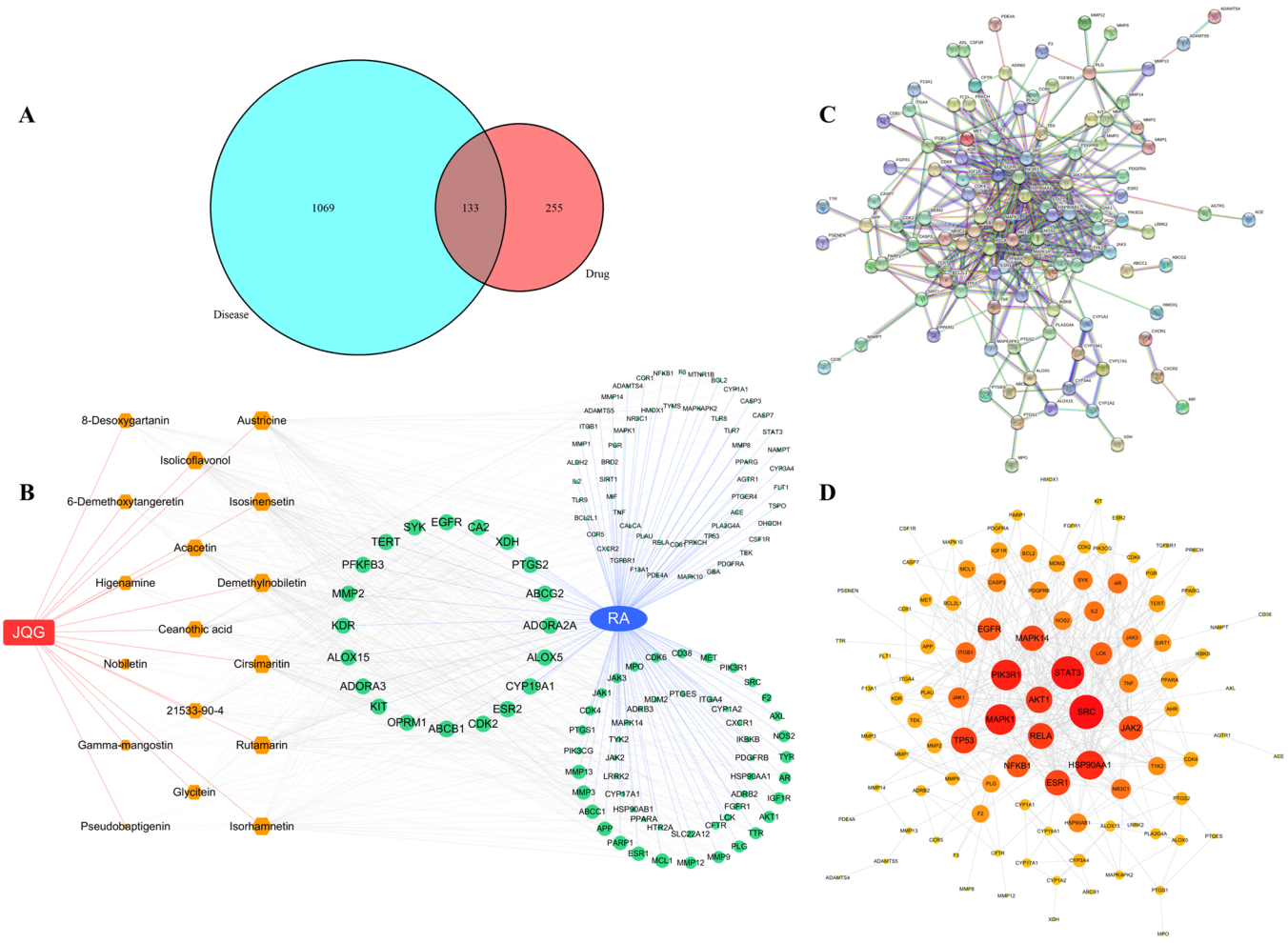

Figure 3. JQG constituent-target-RA network. (A) Intersected target genes of JQG and RA; (B) constituent-target-RA network;(C) protein−protein-interaction (PPI) network of intersected target genes; and (D) PPI network of key target genes based on degree.

ethyl acetate extract (EAE), and n-butanol extract (NBE) were evaluated in RAW264.7-cell lines stimulated by lipopolysaccharide (LPS) to screen the bioactive partition of JQG extract. As shown in Figure 1A−D, nitric oxide (NO), interleukin-6 (IL-6), tumor necrosis factor-alpha (TNF-α), and prostaglandin E2 (PGE2) concentrations were significantly increased after LPS stimulation in the LPS group ($p < 0.001$). EE and NBE could significantly suppress LPS-induced increases in NO, IL-6, TNF-α, and PGE2 levels ($p < 0.05$) at 50 and 100 μg/mL, whereas EAE yielded the best anti-inflammatory effects compared to other partitions that could suppress LPS-induced cytokine increases ($p < 0.01$) at 25 μg/mL. Therefore, EAE was selected for the following experiments.

2.2. Anti-Inflammatory Effects of EAE in Rats. After obtaining the bioactive partition, its anti-arthritis effects were evaluated in adjuvant-induced arthritis (AIA) rats. As shown in Figure 1E, the edema of the left hind paw obviously increased in the model group on the 9th day of injection compared with normal rats ($p < 0.01$). Both EAE and aspirin decreased the edema of the left hind paw after the 15th day of injection, while EAE yielded better effects than aspirin in suppressing the swelling of the left hind paw. After 14 days of administration, EAE significantly ameliorated the swelling of AIA rats and displayed remarkable anti-inflammatory effects via the down-regulation of the inflammatory cytokines IL-1β, TNF-α, and IL-6 ($p < 0.001$) (Figure 1F−H). Moreover, when compared with normal group rats, the model group rats exhibited severe bone erosion and infiltration of immune and inflammatory cells by histological estimation. Furthermore, EAE suppressed the infiltration of inflammatory cells and bone erosion, as shown in Figure 1I. The abovementioned data demonstrated that EAE could attenuate the inflammatory response in RA treatment.

2.3. Constituent Identification in EAE by UPLC-Orbitrap Mass Spectrometry. In this study, an Orbitrap Exploris 120 high-resolution mass spectrometer was used to analyze the active constituents in EAE. A total of 58 constituents were identified in EAE. Representative total ion chromatograms (TICs) of EAE are shown in Figure 2. Subsequently, an oral bioavailability (OB) of ≥30% and drug likeness of ≥0.18[27] obtained from the Traditional Chinese Medicine Systems Pharmacology Database and Analysis Platform were used to screen the potential core constituents. Finally, 17 constituents (6-demethoxytangeretin, 8-desoxygartanin, 21533-90-4 (2′,7-Dihydroxy-4′,5′-dimethoxyisoflavone), acacetin, austricine, ceanothic acid, cirsimaritin, demethylnobiletin, gamma-mangostin, glycitein, higenamine, isolicoflavonol, isorhamnetin, isosinensetin, nobiletin, pseudobaptigenin, and rutamarin) were screened as the core bioactive constituents of JQG for RA treatment.

2.4. JQG Constituent-Target-RA Network. The potential targets of JQG were predicted and collected from the Swiss

https://doi.org/10.1021/acsomega.2c07094
ACS Omega 2023, 8, 2586−2595

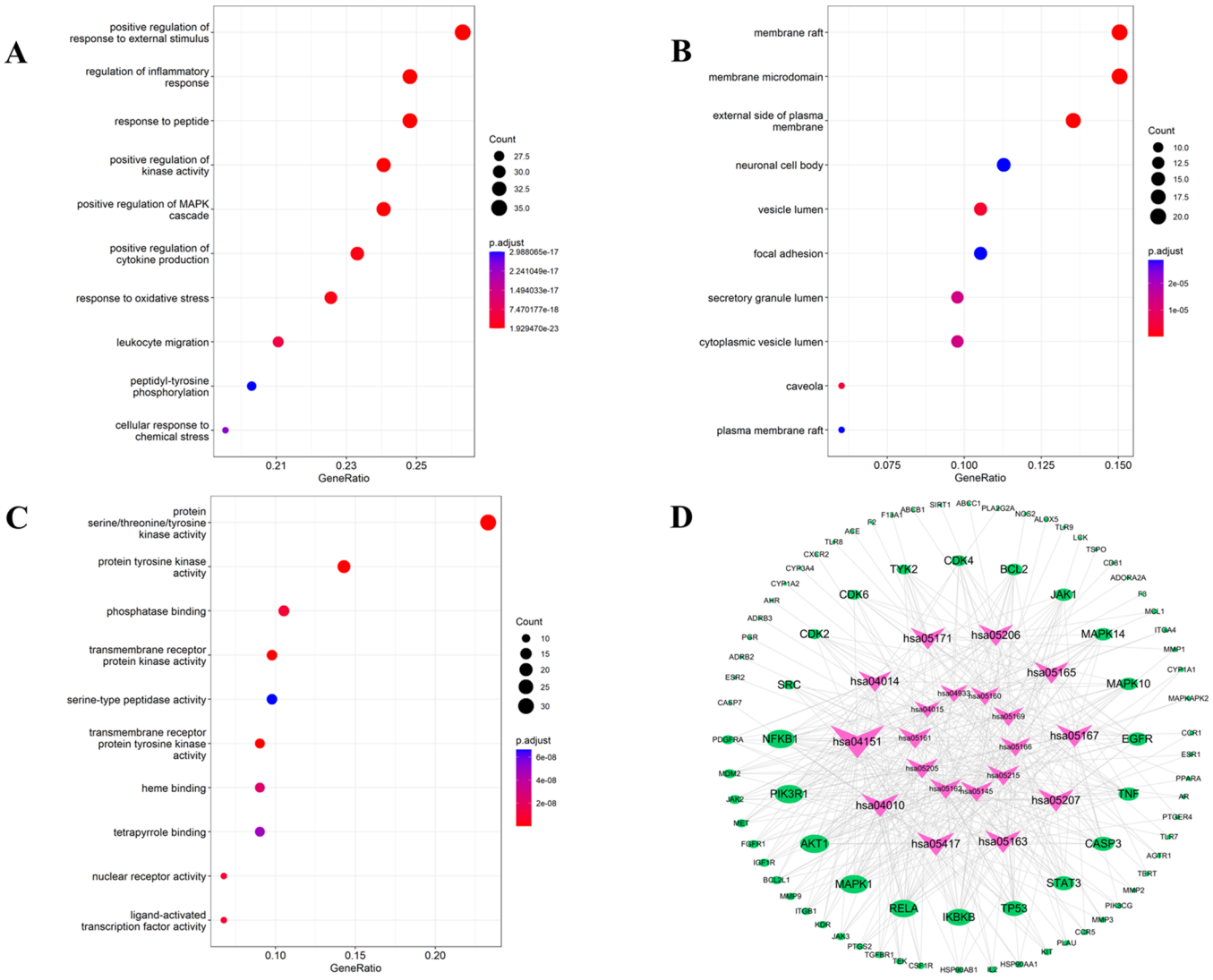

Figure 4. Gene ontology enrichment analysis and KEGG analysis. The top 10 items of (A) biological process and (B) cellular composition, (C) molecular function, and (D) top 20 items of KEGG pathway and core gene topology analysis. The KEGG pathway corresponding to the hsa code is listed in Table S1.

TargetPrediction database and 388 potential targets were obtained after deleting duplicates. The targets of RA were collected from the OMIM, GeneCards, and Therapeutic Target Database databases, and 1202 potential targets were obtained after deleting duplicates. After the intersection between JQG targets and RA targets, a Venn diagram was plotted to obtain 133 intersecting targets (Figure 3A). Then, the intersected targets were imported into Cytoscape software to build the ingredient-target-RA network (Figure 3B). Additionally, the core targets were imported into the STRING database. The protein−protein-interaction (PPI) is displayed in Figure 3C,D. The larger the degree value is, the closer the relationship between proteins. The top 15 targets were SRC, STAT3, MAPK1, PIK3R1, HSP90AA1, AKT1, RELA, TP53, MAPK14, and ESR1 based on degree values.

2.5. GO and KEGG Enrichment Analysis. Based on GO function analysis, the top 10 biological process (BP), cellular composition (CC), and molecular function (MF) entries are displayed in Figure 4A−C. In BP, positive regulation of response to external stimulus, regulation of inflammatory response, and response to oxidative stress were the main items. The top CC items mainly involved membrane rafts, membrane microdomains, and the external side of the plasma membrane. For MF, protein serine/threonine/tyrosine kinase activity, protein tyrosine kinase activity, and transmembrane receptor protein tyrosine kinase activity were the main items. Kyoto Encyclopedia of Genes and Genomes (KEGG) pathway enrichment analysis yielded 151 related signaling pathways, including the PI3K-Akt signaling pathway, MAPK signaling pathway, and NF-kappa B signaling pathway. The top 20 pathways and the interaction of genes and core pathways are shown in Figure 4D (other pathways like ferroptosis are not shown). Among these pathways, the PI3K-Akt signaling pathway, MAPK signaling pathway, NF-kappa B signaling pathway, Toll-like receptor signaling pathway, and AGE-RAGE signaling pathway were associated with inflammation. Additionally, RELA (NF-κB P65) was the top core gene among the key genes MAPK1, NFKB1, PIK3R1, IKBKB, EGFR, AKT1, TP53, CASP3, and STAT3.

2.6. Molecular Docking. The screened core targets were verified by using the molecular operation platform software MOE, which could more intuitively show the optimal

https://doi.org/10.1021/acsomega.2c07094
ACS Omega 2023, 8, 2586−2595

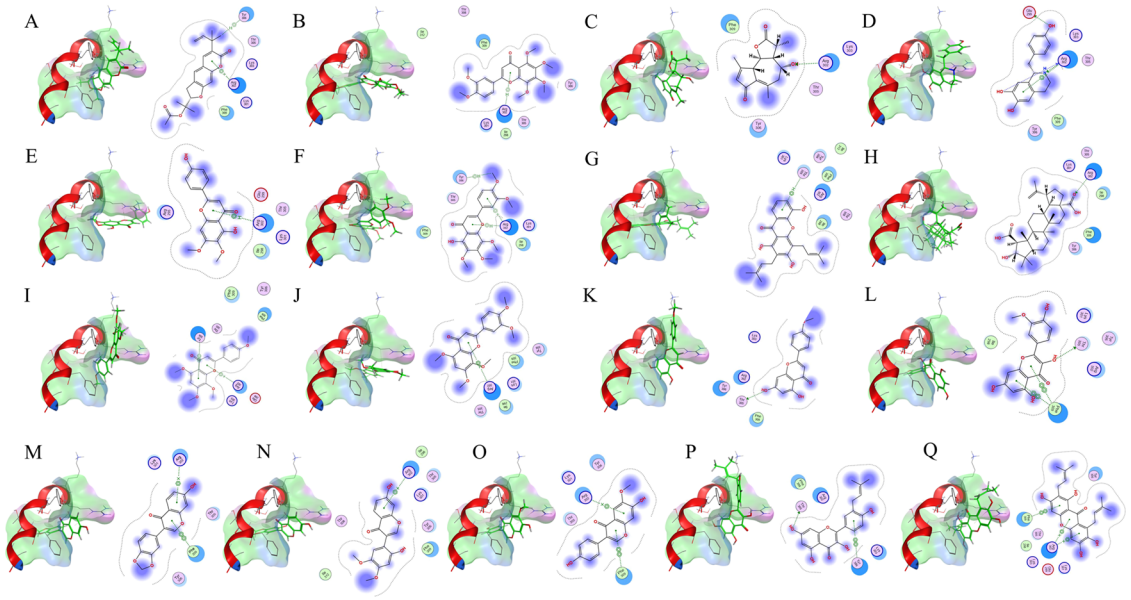

Figure 5. Schematic diagram of the docking results of JQG key constituents with NF-κB P65 (PDB Code 1k3z). (A) rutamarin; (B) nobiletin; (C) austricine; (D) higenamine; (E) cirsimaritin; (F) demethylnobiletin; (G) 8-desoxygartanin; (H) ceanothic acid; (I) 6-demethoxytangeretin; (J) isosinensetin; (K) acacetin; (L) isorhamnetin; (M) pseudobaptigenin; (N) 21533-90-4; (O) glycitein; (P) isolicoflavonol; and (Q) gamma-mangostin.

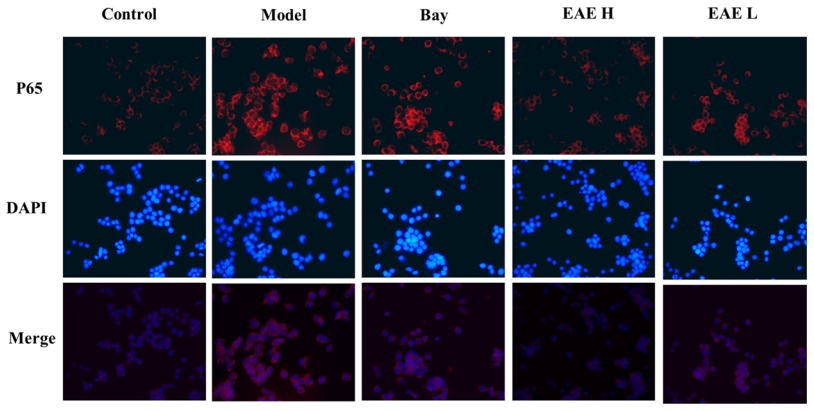

Figure 6. Anti-inflammatory effects of EAE by modulating NF-κB P65 in RAW264.7 cells stimulated with 1 μg/mL LPS (n = 3). EAE significantly reduced NF-κB P65 translocation from the cytoplasm to the nucleus. The doses of EAE L/H and Bay11-7028 were 25/100 μg/mL and 20 μM, respectively.

interaction between the core targets and key constituents. The molecular docking results of RELA (NF-κB P65) with core constituents are given in Table S2. The results showed that there might be hydrogen bonding, pi−cation, pi−pi, pi−H, and other intermolecular binding forces between the active constituent and RELA (NF-κB P65). The binding interaction of core constituents with RELA (NF-κB P65) chain A is shown in Figure 5. Almost all docking scores of core constituents were better than the positive control Nigakinone, indicating good ligand−recepor binding.

2.7. Mechanism Validation for the Anti-Inflammatory Effects of EAE. In the resting state, NF-κB exists in the cytoplasm in an inactive state. When the upstream signal activates NF-κB, it translocates from the cytoplasm to the nucleus (especially NF-κB P65) and interacts with inflammation-related genes to induce inflammation.[28] In this study, we wanted to investigate whether EAE could inhibit NF-κB P65 translocation from the cytoplasm to the nucleus. As shown in Figure 6, NF-κB P65 translocation from the cytoplasm to the nucleus was significantly increased after LPS stimulation in the model group. Bay and EAE significantly suppressed LPS-induced increases in NF-κB P65 in the nucleus, whereas EAE H yielded the strongest negative regulation of NF-κB.

3. DISCUSSION

As a traditional herbal product, JQG is widely used in folk applications for RA treatment. The chemical constituents in JQG are the basis of its pharmacological activity. Due to the development of modern technology, many chemical constituents in JQG have been identified.[29−32] However, which constituent exerts a core pharmacological role, not to mention the exact mechanism for RA treatment, remains unknown. In the present work, we investigated the key constituents and potential mechanisms of JQG for RA treatment.

The chemical constituents in JQG extracts vary depending on the polarity of the extracted solvents, thus resulting in varied pharmacological activities. For example, EAE of JQG yields better antiherpetic activity than other bioactive

https://doi.org/10.1021/acsomega.2c07094
ACS Omega 2023, 8, 2586−2595

partitions extracted by different solvents.[33] In this study, EAE of JQG also displayed better anti-inflammatory effects than other bioactive partitions.

Constituent identification plays a precursor role in network pharmacology analysis for traditional herbal medicine. Varied constituents produce radically different core targets and action pathways. Therefore, an ultra-performance liquid chromatography (UPLC)-Orbitrap mass spectrometer was used to identify bioactive constituents. Consistent with a previous report, the identified constituents mainly belonged to flavonoids, terpenoids, and oligostilbenes. For network analysis, OB, drug-like, and a degree in the constituent-target network were acknowledged rules for screening core active constituents.[6] Thus, these parameters were used to extract the constituents, and anti-inflammatory effects were used to estimate the bioactivity of core constituents. A total of 17 constituents (6-demethoxytangeretin, 8-desoxygartanin, 21533-90-4, acacetin, austricine, ceanothic acid, cirsimaritin, demethylnobiletin, gamma-mangostin, glycitein, higenamine, isolicoflavonol, isorhamnetin, isosinensetin, nobiletin, pseudobaptigenin, and rutamarin) were screened as the core bioactive constituents of JQG for RA treatment. In fact, these core constituents have already demonstrated a clear anti-inflammatory effect according to previous reports.[34−42] Additionally, our results from molecular docking verified the high binding affinity of the key active ingredients to the core target. In summary, the above-reported evidence further strengthened the reliability of screening these compounds as JQG core active constituents for RA treatment.

Several studies have reported that JQG total extract exhibits anti-inflammatory effects via the NF-κB signaling pathway to alleviate osteoarthritis and ulcerative colitis.[18,19] However, there has been almost no mechanistic research on JQG for RA treatment because of its complicated constituents, multiple targets, and multiple pathways. Therefore, the exact treatment mechanism needs to be studied. Here, based on network analysis, the main targets of EAE were affiliated with the PI3K-AKT and MAPK signaling pathways, and these pathways may be involved in immune function, inflammation, and bone erosion.[43−48] Furthermore, these pathways had many intersection genes, and the NF-κB signaling pathway was one of the key overlaps among them. Activation of the PI3K-AKT and MAPK pathways can trigger the NF-κB signaling pathway.[49−53] Moreover, NF-κB plays an important role in immune function, inflammation, and cancer.[54−56] After deduction by network pharmacology, molecular docking was used to explore the potential interaction between NF-κB and key constituents. Molecular docking results indicated good ligand−receptor binding interactions between NF-κB and key constituents. Subsequently, immunofluorescence was used to further verify the interaction between NF-κB and EAE. Consistent with the molecular docking results, EAE significantly reduced NF-κB P65 translocation from the cytoplasm to the nucleus. In summary, these results suggested that EAE could suppress the NF-κB pathway to exert anti-inflammatory effects, which, thus, contribute to the efficacy of JQG for RA therapy.

4. MATERIALS AND METHODS

4.1. Chemicals and Reagents. Raw JQG materials were obtained from Tong Ren Tang Co Ltd. (Hefei, China). Analytical grade ethanol, petroleum ether, chloroform, ethyl acetate, and n-butanol were obtained from Hefei Baierdi Chemical Technology Co Ltd. Primary antibodies against P65 were purchased from Abcam Trading Co. Ltd. (Shanghai, China). Enzyme-linked immunosorbent assay (ELISA) kits for IL-6, TNF-α, and IL-1β were purchased from Multisciences (Lianke) Biotech Co Ltd. (Hangzhou, China), and mouse PGE2 was purchased from Jianglai Biotechnology Co Ltd. (Shanghai, China). Mouse macrophage RAW264.7-cell lines were obtained from ATCC (Passage 20−25, American Type Culture Collection, Rockville, MD, USA). Liquid chromatography (LC)/mass spectrometry (MS)-grade methanol was acquired from Merck (Merck KGaA, Darmstadt, Germany). All other used reagents were of analytical grade and were obtained from commercial sources.

4.2. Preparation of JQG Extract. JQG powder (10 kg) was extracted with 80% ethanol (80 L) three times at ambient temperature, and the filtrate was concentrated under reduced pressure to obtain the EE residue. Then, the residue was dissolved in water and successively partitioned by petroleum ether, chloroform, ethyl acetate, and n-butanol (2.5 L). Then, the organic phase was removed by a rotary vacuum evaporator, and the extract was dried by a vacuum freeze drier. Finally, 800.28 g of EE, 18.21 g ofPEE, 12.95 g of CE, 41.43 g of EAE, and 19.39 g of NBE were obtained.

4.3. Screening of Bioactive Partition of JQG Extract. RAW264.7 cells were seeded on 24-well plates (7×10^4 cells/well) in Dulbecco's modified Eagle's medium (DMEM) for 24 h. Extracts partitioned by ethanol, petroleum ether, chloroform, ethyl acetate, and n-butanol extraction were added to the medium, and the cells were incubated for 1 h before stimulation with LPS (1 μg/mL) for 23 h. After the treatment, the cell supernatant was collected and centrifuged at 4 °C and 20,817 *g* for 10 min. Then, the supernatant was collected to detect the concentration of NO, IL-6, TNF-α, and PGE2 using ELISA kits. By comparing the effects of these partitioned extracts on inflammatory mediators, the partition with the best efficacy was selected for the following study.

4.4. Anti-Arthritis Effects of JQG Extract. In this study, the animal experiment was approved by the Ethics Review Committee for Animal Experimentation of Anhui Medical University. AIA of rats was induced according to a previous study.[57] Briefly, 0.1 mL of heat-killed Bacillus Calmette−Guérin in liquid paraffin was intradermally injected into the right hind paw of Sprague Dawley rats (male, 160−180 g). The EAE of JQG was dissolved in sodium carboxymethyl cellulose (CMC-Na). Prior to the onset of AIA, animals were randomly divided into four groups ($n = 5$), including the normal group (CMC-Na as a vehicle), model group (CMC-Na as a vehicle), EAE group (200 mg/kg/day), and aspirin group (50 mg/kg/day). Rat paw volumes were measured on day 0 and day 9. Then, paw volumes were measured every 6 days. On day 28 after treatment, animals were killed, and a rat ankle joint was used for histological examination. Rat serum was used for the measurement of inflammatory cytokines, including TNF-α, IL-6, and IL-1β, according to the manufacturer's instructions.

4.5. Qualitative Analysis of Phytochemical Constituents in EAE of JQG. Qualitative analysis of phytochemical constituents was performed on a UPLC system coupled with an Orbitrap Exploris 120 mass spectrometer (Vanquish, Thermo Fisher Scientific). Constituent separation was achieved on a Waters UPLC BEH C18 column (2.1 mm ID × 100 mm, 1.7 μm). The mobile phases consisted of A (0.1% formic acid) and B (methanol-containing formic acid), with a flow rate of 0.5 mL/min, using a gradient elution of 15−75% B at 0−11 min, 75−98% B at 11−12 min, 98% B at 12−14 min,

https://doi.org/10.1021/acsomega.2c07094
ACS Omega 2023, 8, 2586−2595

98−15% B at 14−14.1 min, and 15% B at 14.1−16 min. An Orbitrap Exploris 120 mass spectrometer was used to analyze the MS and MS/MS data under IDA (information-dependent acquisition) mode in both positive and negative modes. The optimal parameters are as follows: sheath gas = 35 Arb; aux gas flow = 15 Arb; ion transfer tube and vaporizer temperature = 350 °C; full ms resolution = 60,000 and MS/MS resolution = 15,000; 16/32/48 voltage collision energy in NCE mode; and spray voltage = 5.5 kV in ESI+ mode or −4 kV in ESI− mode. The constituents were identified by matching their average retention times, molecular ions, and product ions with the developed database by Biotree Biotech (Shanghai, China).

4.6. Construction of the Active Constituent-Target-RA Network. PubChem (https://pubchem.ncbi.nlm.nih.gov) was used to obtain the structures of the active constituents of JQG, which were imported into Swiss Target Prediction (http://www.swisstargetprediction.ch) to predict the corresponding targets of the active components. The OMIM database (https://www.omim.org), GeneCards database (https://www.genecards.org), and TherapeuticTarget database (http://db.idrblab.net/ttd) were used to screen RA-relevant target genes by setting the species as *Homo sapiens* (*H. sapiens*). Finally, target genes obtained from the three databases were sorted to remove duplicates to obtain the final targets. The obtained targets of JQG and the relevant target genes of RA were intersected, and a Venn diagram was drawn. The intersection targets were regarded as potential action targets of the core active constituents of JQG in RA treatment. The intersection targets were imported into Cytoscape 3.7.1 software to construct an active constituent-target-RA network. The obtained intersection targets were also imported into the String database (https://www.string-db.org) for predicting PPIs with species set as *H. sapiens*, and the targets with a binding score of ≥0.9 were screened out. Then, the screened targets were imported into Cytoscape 3.7.1 software to obtain a visual PPI network diagram.

4.7. Enrichment Analysis. The obtained intersection targets were imported into the Bioconductor database (http://www.bioconductor.org) for gene ontology (GO) and KEGG analysis. GO analysis included MF, BP, and CC, and a p of <0.05 was regarded as the screening criterion. The top 20 items from GO biological function analysis and KEGG pathway enrichment analysis were plotted into a histogram and bubble picture for visual analysis, respectively.

4.8. Molecular Docking. The molecular operating platform software MOE (molecule operating environment) was used for docking. The three-dimensional structure of the target protein was downloaded from the RCSB-PDB database (http://www.pdb.org). The corresponding ligands were prepared from the PubChem database (https://pubchem.ncbi.nlm.nih.gov). Using the MOE-Dock module, semiflexible docking between the ligand and the receptor was performed. The triangle matcher scoring function was selected as the placement function, and London dG was selected as the scoring function. Additionally, the smaller the score value achieved, the more stable the ligand−receptor binding would be.

4.9. Mechanism Validation Based on Immunofluorescence. RAW264.7 cells were seeded on 24-well plates containing glass coverslips at a density of 7×10^4 cells/well in DMEM overnight. Then, the medium containing EAE or Bay11-7082 was added, and the cells were incubated for 1 h before stimulation with LPS (1 μg/mL) for 23 h. After the treatment, the cells were fixed with paraformaldehyde for 15 min, permeabilized with Triton X-100 for 20 min, and incubated with 5% bovine serum albumin for 30 min. Next, the cells were incubated with primary antibodies overnight at 4 °C, secondary antibodies for 30 min at room temperature, and DAPI for 5 min. Finally, the cells on the glass coverslip were visualized by a fluorescence microscope.

4.10. Statistical Analysis. All results were displayed as the mean ± standard deviation, and a one-way analysis of variance was used between groups by GraphPad Software (Prism 9, San Diego, CA, USA). A p of <0.05 was considered statistically significant.

5. CONCLUSIONS

EAE yielded the best anti-inflammatory effects in vitro and in vivo among JQG extracts. By UPLC coupled Orbitrap mass spectrometer analysis, a total of 58 constituents were identified, and 17 constituents were regarded as the core constituents for the anti-inflammatory effects. The therapeutic efficacy of EAE in RA might be achieved by blocking the NF-κB signaling pathway. The inspiring results presented above indicated that core constituents represent a promising herbal product for RA treatment and is worth further investigation.

■ ASSOCIATED CONTENT

Supporting Information

The Supporting Information is available free of charge at https://pubs.acs.org/doi/10.1021/acsomega.2c07094.

The KEGG pathway corresponding to the hsa code and docking scores of core constituents of JQG with NF-κB P65 (PDB Code 1k3z) (PDF)

■ AUTHOR INFORMATION

Corresponding Authors

Wei Hu − *Department of Clinical Pharmacology, The Second Hospital of Anhui Medical University, Hefei 230601, China; Anhui Provincial Institute of Translational Medicine, Hefei 230032, China*; Email: huwei@ahmu.edu.cn

Chao Lu − *First Affiliated Hospital, Anhui University of Science & Technology, Huainan 232001, China*; Email: luchao@aust.edu.cn

Authors

Biao Qu − *Department of Clinical Pharmacology, The Second Hospital of Anhui Medical University, Hefei 230601, China; Anhui Provincial Institute of Translational Medicine, Hefei 230032, China*; orcid.org/0000-0001-8615-8666

Shimin Wang − *Fuyang Fifth People's Hospital, Fuyang 236063, China*

Hailan Zhu − *College of Pharmacy, School of Zhejiang University of Technology, Hangzhou 310014, China*

Tianpeng Yin − *Department of Bioengineering, Zunyi Medical University, Zhuhai 519041, China*

Renpeng Zhou − *Department of Clinical Pharmacology, The Second Hospital of Anhui Medical University, Hefei 230601, China; Anhui Provincial Institute of Translational Medicine, Hefei 230032, China*

Complete contact information is available at: https://pubs.acs.org/10.1021/acsomega.2c07094

Author Contributions

†B.Q., S.W., and H.Z. contributed equally to this work.

https://doi.org/10.1021/acsomega.2c07094
ACS Omega 2023, 8, 2586−2595

Notes

The authors declare no competing financial interest.

■ ACKNOWLEDGMENTS

This article was financially supported by the National Natural Science Foundation of China (Grant no. 82071591), Key Projects of Administration of Traditional Chinese Medicine of Anhui Province (Grant no. 2020cczd05), National Natural Science Foundation of Anhui Province (Grant no. 1908085QH317), and National Natural Science Foundation Incubation Program of The Second Hospital of Anhui Medical University (Grant no. 2019GMFY03;2022GMFY08).

■ ABBREVIATIONS

JQG, Jin Quegen
RA, rheumatoid arthritis
AIA, adjuvant-induced arthritis
EAE, ethyl acetate extract
UPLC, ultra-performance liquid chromatography
OB, oral bioavailability
DL, drug-like
NF-κB, nuclear factor kappa B
DMARD, disease-modifying anti-rheumatic drug
ELISA, enzyme-linked immunosorbent assay
IL, interleukin
TNF, tumor necrosis factor
PGE2, prostaglandin E2
EE, ethanol extract
PEE, petroleum ether extract
CE, chloroform extract
NBE, n-butanol extract
DMEM, Dulbecco's modified Eagle's medium
LPS, lipopolysaccharide
NO, nitric oxide
CMC-Na, sodium carboxymethyl cellulose
PPI, protein−protein interaction
GO, Gene Ontology
KEGG, Kyoto Encyclopedia of Genes and Genomes
MF, molecular function
BP, biological process
CC, cellular composition
MOE, molecule operating environment
TICs, total ion chromatograms

■ REFERENCES

(1) Chen, Z.; Li, X. P.; Li, Z. J.; Xu, L.; Li, X. M. Reduced hepatotoxicity by total glucosides of paeony in combination treatment with leflunomide and methotrexate for patients with active rheumatoid arthritis. *Int. Immunopharmacol.* **2013**, *15*, 474−477.
(2) Smolen, J. S.; Aletaha, D.; McInnes, I. B. Rheumatoid arthritis. *Lancet* **2016**, *388*, 2023−2038.
(3) Cojocaru, M.; Cojocaru, I. M.; Silosi, I.; Vrabie, C. D.; Tanasescu, R. Extra-articular Manifestations in Rheumatoid Arthritis. *Maedica (Bucur)* **2010**, *5*, 286−291.
(4) Burmester, G. Advances in diagnosis, treatment and definition of remission. *Nat. Rev. Rheumatol.* **2012**, *8*, 65−66.
(5) Saag, K. G.; Teng, G. G.; Patkar, N. M.; Anuntiyo, J.; Finney, C.; Curtis, J. R.; Paulus, H. E.; Mudano, A.; Pisu, M.; Elkins-Melton, M.; et al. American College of Rheumatology 2008 recommendations for the use of nonbiologic and biologic disease-modifying antirheumatic drugs in rheumatoid arthritis. *Arthritis Rheum.* **2008**, *59*, 762−784.
(6) Li, Z.; Qu, B.; Zhou, L.; Chen, H.; Wang, J.; Zhang, W.; Chen, C. A New Strategy to Investigate the Efficacy Markers Underlying the Medicinal Potentials of s Benth. *Front. Pharmacol.* **2021**, *12*, No. 748684.
(7) Bauer, A.; Brönstrup, M. Industrial natural product chemistry for drug discovery and development. *Nat. Prod. Rep.* **2014**, *31*, 35−60.
(8) Hopkins, A. L. Network pharmacology. *Nat. Biotechnol.* **2007**, *25*, 1110−1111.
(9) Yu, J.; Xiao, Z.; Zhao, R.; Lu, C.; Zhang, Y. Paeoniflorin suppressed IL-22 via p38 MAPK pathway and exerts anti-psoriatic effect. *Life Sci.* **2017**, *180*, 17−22.
(10) Zhou, Y.; Jin, L.; Kong, F.; Zhang, H.; Fang, X.; Chen, Z.; Wang, G.; Li, X.; Li, X. Clinical and immunological consequences of total glucosides of paeony treatment in Sjogren's syndrome: A randomized controlled pilot trial. *Int. Immunopharmacol.* **2016**, *39*, 314−319.
(11) Jeong, W.; Ahn, E.-K.; Oh, J. S.; Hong, S. S. Caragasinin C: a new oligostilbene from the roots of *Caragana sinica*. *J. Asian Nat. Prod. Res.* **2017**, *19*, 1143−1147.
(12) Kitanaka, S.; Ikezawa, T.; Yasukawa, K.; Yamanouchi, S.; Takido, M.; Sung, H. K.; Kim, I. H. (+)-Alpha-viniferin, an anti-inflammatory compound from Caragana chamlagu root. *Chem. Pharm. Bull.* **1990**, *38*, 432−435.
(13) Meng, Q.; Niu, Y.; Niu, X.; Roubin, R. H.; Hanrahan, J. R. Ethnobotany, phytochemistry and pharmacology of the genus Caragana used in traditional Chinese medicine. *J. Ethnopharmacol.* **2009**, *124*, 350−368.
(14) Du, X.; Guo, X.; Guo, C.; Guo, Z.; He, C. Clinical research of *Caragana sinica root* for rheumatoid arthritis. *J. Med. Pharma. Chin. Minorit.* **1998**, *2*, 11−13.
(15) Zhang, W.; Zhang, C. Discussion of aspirin, glucocorticoids and *Caragana sinica root* in the treatment of rheumatoid arthritis. *J. Baotou. Med.* **1994**, *18*, 14.
(16) Jin, Q.; Han, X. H.; Hong, S. S.; Lee, C.; Choe, S.; Lee, D.; Kim, Y.; Hong, J. T.; Lee, M. K.; Hwang, B. Y. Antioxidative oligostilbenes from *Caragana sinica*. *Bioorg. Med. Chem. Lett.* **2012**, *22*, 973−976.
(17) Lee, S. R.; Kwak, J. H.; Kim, H. J.; Pyo, S. Neuroprotective effects of kobophenol A against the withdrawal of tropic support, nitrosative stress, and mitochondrial damage in SH-SY5Y neuroblastoma cells. *Bioorg. Med. Chem. Lett.* **2007**, *17*, 1879−1882.
(18) Li, T.; Zou, Q.-P.; Huang, F.; Cheng, G.-G.; Mao, Z.-W.; Wang, T.; Dong, F.-W.; Li, B.-J.; He, H.-P.; Li, Y.-P. Flower extract of. ameliorates DSS-induced ulcerative colitis by affecting TLR4/NF-B and TLR4/MAPK signaling pathway in a mouse model. *Iran. J. Basic Med. Sci.* **2021**, *24*, 595−603.
(19) Min, G.-Y.; Park, J.-M.; Joo, I.-H.; Kim, D.-H. Inhibition effect of extracts on Osteoarthritis through MAPKs, NF-κB signaling pathway. *Int. J. Med. Sci.* **2021**, *18*, 861−872.
(20) Sung, S. H.; Kang, S. Y.; Lee, K. Y.; Park, M. J.; Kim, J. H.; Park, J. H.; Kim, Y. C.; Kim, J.; Kim, Y. C. (+)-Alpha-viniferin, a stilbene trimer from Caragana chamlague, inhibits acetylcholinesterase. *Biol. Pharm. Bull.* **2002**, *25*, 125−127.
(21) Kulanthaivel, P.; Janzen, W. P.; Ballas, L. M.; Jiang, J. B.; Hu, C. Q.; Darges, J. W.; Seldin, J. C.; Cofield, D. J.; Adams, L. M. Naturally occurring protein kinase C inhibitors; II. Isolation of oligomeric stilbenes from *Caragana sinica*. *Planta Med.* **1995**, *61*, 41−44.
(22) Lee, S.-R.; Kwak, J.-H.; Park, D.-S.; Pyo, S. Protective effect of kobophenol A on nitric oxide-induced cell apoptosis in human osteoblast-like MG-63 cells: involvement of JNK, NF-κB and AP-1 pathways. *Int. Immunopharmacol.* **2011**, *11*, 1251−1259.
(23) Kitanaka, S.; Takido, M.; Mizoue, K.; Nakaike, S. Cytotoxic cardenolides from woods of Euonymus alata. *Chem. Pharm. Bull.* **1996**, *44*, 615−617.
(24) Li, S.; Zhang, B. Traditional Chinese medicine network pharmacology: theory, methodology and application. *Chin. J. Nat. Med.* **2013**, *11*, 110−120.
(25) Hopkins, A. L. Network pharmacology: the next paradigm in drug discovery. *Nat. Chem. Biol.* **2008**, *4*, 682−690.
(26) Nogales, C.; Mamdouh, Z. M.; List, M.; Kiel, C.; Casas, A. I.; Schmidt, H. H. H. W. Network pharmacology: curing causal

https://doi.org/10.1021/acsomega.2c07094
ACS Omega 2023, 8, 2586−2595

mechanisms instead of treating symptoms. *Trends Pharmacol. Sci.* **2022**, *43*, 136−150.
(27) Wu, J.; Hong, S.; Xie, X.; Liu, W. A Network Pharmacology-Based Study on the Anti-Lung Cancer Effect of Dipsaci Radix. *Evid. Based Complement. Alternat. Med.* **2020**, *2020*, No. 7424061.
(28) Kracht, M.; Müller-Ladner, U.; Schmitz, M. L. Mutual regulation of metabolic processes and proinflammatory NF-κB signaling. *J. Allergy Clin. Immunol.* **2020**, *146*, 694−705.
(29) Chen, G.; Luo, H.; Ye, J.; Hu, C. Determination of hypaphorine and oligomeric stilbenes in the root of *Caragana sinica* by capillary electrophoresis with electrochemical detection. *Talanta* **2001**, *54*, 1067−1076.
(30) Yang, G. X.; Zhou, J. T.; Li, Y. Z.; Hu, C. Q. Anti-HIV bioactive stilbene dimers of Caragana rosea. *Planta Med.* **2005**, *71*, 569−571.
(31) Wang, S. G.; Ma, D. Y.; Hu, C. Q. Two new oligostilbenes from *Caragana sinica*. *J. Asian Nat. Prod. Res.* **2004**, *6*, 241−248.
(32) Liu, H.-X.; Lin, W.-H.; Yang, J.-S. Oligomeric stilbenes from the root of Caragana stenophylla. *Chem. Pharm. Bull.* **2004**, *52*, 1339−1341.
(33) Woo, E. R.; Kim, H. J.; Kwak, J. H.; Lim, Y. K.; Park, S. K.; Kim, H. S.; Lee, C. K.; Park, H. Anti-herpetic activity of various medicinal plant extracts. *Arch. Pharmacal Res.* **1997**, *20*, 58−67.
(34) Singh, S.; Gupta, P.; Meena, A.; Luqman, S. Acacetin, a flavone with diverse therapeutic potential in cancer, inflammation, infections and other metabolic disorders. *Food Chem. Toxicol.* **2020**, *145*, No. 111708.
(35) Sreeja, P.S.; Arunachalam, K.; Martins, D.T.D.O.; Lima, J.C.D.S.; Balogun, S.O.; Pavan, E.; Saikumar, S.; Dhivya, S.; Kasipandi, M.; Parimelazhagan, T. Sphenodesme involucrata var. paniculata (C.B. Clarke) Munir.: Chemical characterization, anti-nociceptive and anti-inflammatory activities of methanol extract of leaves. *J. Ethnopharmacol.* **2018**, *225*, 71−80.
(36) Yan, H.; Wang, H.; Ma, L.; Ma, X.; Yin, J.; Wu, S.; Huang, H.; Li, Y. Cirsimaritin inhibits influenza A virus replication by downregulating the NF-κB signal transduction pathway. *Virol. J.* **2018**, *15*, 88.
(37) Bas, E.; Recio, M. C.; Giner, R. M.; Máñez, S.; López-Ginés, C.; Gil-Benso, R.; Ríos, J. L. Demethylnobiletin inhibits delayed-type hypersensitivity reactions, human lymphocyte proliferation and cytokine production. *Br. J. Pharmacol.* **2007**, *152*, 1272−1282.
(38) Chiu, Y.-S.; Wu, J.-L.; Yeh, C.-T.; Yadav, V. K.; Huang, H.-S.; Wang, L.-S. γ-Mangostin isolated from L. suppresses inflammation and alleviates symptoms of osteoarthritis via modulating miR-124-3p/IL-6/NF-κB signaling. *Aging* **2020**, *12*, 6630−6643.
(39) Takaoka, O.; Mori, T.; Ito, F.; Okimura, H.; Kataoka, H.; Tanaka, Y.; Koshiba, A.; Kusuki, I.; Shigehiro, S.; Amami, T.; et al. Daidzein-rich isoflavone aglycones inhibit cell growth and inflammation in endometriosis. *J. Steroid Biochem. Mol. Biol.* **2018**, *181*, 125−132.
(40) Bai, X.; Ding, W.; Yang, S.; Guo, X. Higenamine inhibits IL-1β-induced inflammation in human nucleus pulposus cells. *Biosci. Rep.* **2019**, *39*, No. BSR20190857.
(41) Ren, X.; Han, L.; Li, Y.; Zhao, H.; Zhang, Z.; Zhuang, Y.; Zhong, M.; Wang, Q.; Ma, W.; Wang, Y. Isorhamnetin attenuates TNF-α-induced inflammation, proliferation, and migration in human bronchial epithelial cells via MAPK and NF-κB pathways. *Anat. Rec. (Hoboken)* **2021**, *304*, 901−913.
(42) Rong, X.; Xu, J.; Jiang, Y.; Li, F.; Chen, Y.; Dou, Q. P.; Li, D. Citrus peel flavonoid nobiletin alleviates lipopolysaccharide-induced inflammation by activating IL-6/STAT3/FOXO3a-mediated autophagy. *Food Funct.* **2021**, *12*, 1305−1317.
(43) Zhou, F.; Mei, J.; Han, X.; Li, H.; Yang, S.; Wang, M.; Chu, L.; Qiao, H.; Tang, T. Kinsenoside attenuates osteoarthritis by repolarizing macrophages through inactivating NF-B/MAPK signaling and protecting chondrocytes. *Acta. Pharm. Sin. B.* **2019**, *9*, 973−985.
(44) Ren, Q.; Guo, F.; Tao, S.; Huang, R.; Ma, L.; Fu, P. Flavonoid fisetin alleviates kidney inflammation and apoptosis via inhibiting Src-mediated NF-κB p65 and MAPK signaling pathways in septic AKI mice. *Biomed. Pharmacother.* **2020**, *122*, No. 109772.
(45) Arthur, J. S. C.; Ley, S. C. Mitogen-activated protein kinases in innate immunity. *Nat. Rev. Immunol.* **2013**, *13*, 679−692.
(46) O'Donnell, J. S.; Massi, D.; Teng, M. W. L.; Mandala, M. PI3K-AKT-mTOR inhibition in cancer immunotherapy, redux. *Semin. Cancer Biol.* **2018**, *48*, 91−103.
(47) Feng, F.-B.; Qiu, H.-Y. Effects of Artesunate on chondrocyte proliferation, apoptosis and autophagy through the PI3K/AKT/mTOR signaling pathway in rat models with rheumatoid arthritis. *Biomed. Pharmacother.* **2018**, *102*, 1209−1220.
(48) Li, S.-T.; Dai, Q.; Zhang, S.-X.; Liu, Y.-J.; Yu, Q.-Q.; Tan, F.; Lu, S.-H.; Wang, Q.; Chen, J.-W.; Huang, H.-Q.; et al. Ulinastatin attenuates LPS-induced inflammation in mouse macrophage RAW264.7 cells by inhibiting the JNK/NF-κB signaling pathway and activating the PI3K/Akt/Nrf2 pathway. *Acta Pharmacol. Sin.* **2018**, *39*, 1294−1304.
(49) Torrealba, N.; Vera, R.; Fraile, B.; Martínez-Onsurbe, P.; Paniagua, R.; Royuela, M. TGF-β/PI3K/AKT/mTOR/NF-kB pathway. Clinicopathological features in prostate cancer. *Aging Male* **2020**, *23*, 801−811.
(50) Yang, H.-L.; Thiyagarajan, V.; Shen, P.-C.; Mathew, D. C.; Lin, K.-Y.; Liao, J.-W.; Hseu, Y.-C. Anti-EMT properties of CoQ0 attributed to PI3K/AKT/NFKB/MMP-9 signaling pathway through ROS-mediated apoptosis. *J. Exp. Clin. Cancer Res.* **2019**, *38*, 186.
(51) Zhao, H.; Wu, L.; Yan, G.; Chen, Y.; Zhou, M.; Wu, Y.; Li, Y. Inflammation and tumor progression: signaling pathways and targeted intervention. *Sig. Transduct. Target. Ther.* **2021**, *6*, 263.
(52) Wang, M.; Xu, H.; Chong Lee Shin, O. L.-S.; Li, L.; Gao, H.; Zhao, Z.; Zhu, F.; Zhu, H.; Liang, W.; Qian, K.; et al. Compound α-keto acid tablet supplementation alleviates chronic kidney disease progression via inhibition of the NF-kB and MAPK pathways. *J. Transl. Med.* **2019**, *17*, 122.
(53) Liu, Z.; Huang, Y.; Jiao, Y.; Chen, Q.; Wu, D.; Yu, P.; Li, Y.; Cai, M.; Zhao, Y. Polystyrene nanoplastic induces ROS production and affects the MAPK-HIF-1/NFkB-mediated antioxidant system in Daphnia pulex. *Aquat. Toxicol.* **2020**, *220*, No. 105420.
(54) Chen, S.; Jiang, S.; Zheng, W.; Tu, B.; Liu, S.; Ruan, H.; Fan, C. RelA/p65 inhibition prevents tendon adhesion by modulating inflammation, cell proliferation, and apoptosis. *Cell Death Dis.* **2017**, *8*, No. e2710.
(55) Indukuri, R.; Hases, L.; Archer, A.; Williams, C. Estrogen Receptor Beta Influences the Inflammatory p65 Cistrome in Colon Cancer Cells. *Front. Endocrinol.* **2021**, *12*, No. 650625.
(56) Zarate, M. A.; Nguyen, L. M.; De Dios, R. K.; Zheng, L.; Wright, C. J. Maturation of the Acute Hepatic TLR4/NF-κB Mediated Innate Immune Response Is p65 Dependent in Mice. *Front. Immunol.* **2020**, *11*, 1892.
(57) Wang, Y.; Han, C.-C.; Cui, D.; Luo, T.-T.; Li, Y.; Zhang, Y.; Ma, Y.; Wei, W. Immunomodulatory Effects of CP-25 on Splenic T Cells of Rats with Adjuvant Arthritis. *Inflammation* **2018**, *41*, 1049−1063.

https://doi.org/10.1021/acsomega.2c07094
ACS Omega 2023, 8, 2586−2595